

MIT Open Access Articles

Gellan gum microgel-reinforced cell-laden gelatin hydrogels

The MIT Faculty has made this article openly available. **Please share** how this access benefits you. Your story matters.

Citation: Shin, Hyeongho, Bradley D. Olsen, and Ali Khademhosseini. "Gellan Gum Microgel-Reinforced Cell-Laden Gelatin Hydrogels." *J. Mater. Chem. B* 2, no. 17 (2014): 2508–2516.

As Published: <http://dx.doi.org/10.1039/c3tb20984a>

Publisher: Royal Society of Chemistry

Persistent URL: <http://hdl.handle.net/1721.1/101210>

Version: Author's final manuscript: final author's manuscript post peer review, without publisher's formatting or copy editing

Terms of use: Creative Commons Attribution-Noncommercial-Share Alike





Published in final edited form as:

J Mater Chem B Mater Biol Med. 2014 May 7; 2(17): 2508–2516. doi:10.1039/C3TB20984A.

Gellan gum microgel-reinforced cell-laden gelatin hydrogels

Hyeongho Shin^{a,b}, Bradley D. Olsen^c, and Ali Khademhosseini^{b,d,e,*}

^aDepartment of Materials Science and Engineering, Massachusetts Institute of Technology, Cambridge, MA 02139, USA

^bCenter for Biomedical Engineering, Department of Medicine, Brigham and Women's Hospital, Harvard Medical School, Cambridge, MA 02139, USA

^cDepartment of Chemical Engineering, Massachusetts Institute of Technology, Cambridge, MA 02139, USA

^dHarvard-MIT Division of Health Sciences and Technology, Massachusetts Institute of Technology, Cambridge, MA 02139, USA

^eWyss Institute for Biologically Inspired Engineering, Harvard University, Boston, MA 02115, USA

Abstract

The relatively weak mechanical properties of hydrogels remain a major drawback for their application as load-bearing tissue scaffolds. Previously, we developed cell-laden double-network (DN) hydrogels that were composed of photocrosslinkable gellan gum (GG) and gelatin. Further research into the materials as tissue scaffolds determined that the strength of the DN hydrogels decreased when they were prepared at cell-compatible conditions, and the encapsulated cells in the DN hydrogels did not function as well as they did in gelatin hydrogels. In this work, we developed microgel-reinforced (MR) hydrogels from the same two polymers, which have better mechanical strength and biological properties in comparison to the DN hydrogels. The MR hydrogels were prepared by incorporating stiff GG microgels into soft and ductile gelatin hydrogels. The MR hydrogels prepared at cell-compatible conditions exhibited higher strength than the DN hydrogels and the gelatin hydrogels, the highest strength being 2.8 times that of the gelatin hydrogels. MC3T3-E1 preosteoblasts encapsulated in MR hydrogels exhibited as high metabolic activity as in gelatin hydrogels, which is significantly higher than that in the DN hydrogels. The measurement of alkaline phosphatase (ALP) activity and the amount of mineralization showed that osteogenic behavior of MC3T3-E1 cells was as much facilitated in the MR hydrogels as in the gelatin hydrogels, while it was not as much facilitated in the DN hydrogels. These results suggest that the MR hydrogels could be a better alternative to the DN hydrogels and have great potential as load-bearing tissue scaffolds.

1. Introduction

Natural tissues have various mechanical properties according to their functions. Tissues such as cartilage, tendon, and bone have great strength because they have to sustain large loads every day. Tissue engineering scaffolds for such load-bearing tissues must therefore have high strength to keep their integrity after being implanted to the load-bearing positions. In this regard, the mechanical weakness of most hydrogels is a major limitation, although they have been considered as a promising candidate for tissue scaffolds due to their advantages such as high water content, permeability, biocompatibility, and ability to encapsulate cells in a three-dimensional environment.¹⁻³ Several new platform materials have been developed to improve the mechanical strength of hydrogels, such as double-network (DN) hydrogels⁴⁻⁶, polyrotaxane hydrogels⁷, nanocomposite hydrogels⁸, ideally homogeneous tetra-PEG hydrogels⁹, ionically cross-linked triblock copolymer hydrogels¹⁰, and shear thinning protein hydrogels reinforced by block copolymer self-assembly¹¹.

Previously we developed cell-laden DN hydrogels by using a cell-compatible two-step photocrosslinking method.¹² Photocrosslinkable gellan gum (GG) was used to make the stiff first network, and photocrosslinkable gelatin was used to make the soft and ductile second network. The strengthening mechanism of DN hydrogels was elucidated that the first network works as a stiff scaffold that sustains the stress throughout the construct, and the soft and ductile second network dissipates the crack energy preventing the failure of the construct.¹³ We adapted this strategy for making cell-laden hydrogels from two photocrosslinkable biomacromolecules. The resulting DN hydrogels exhibited significantly higher strength than single network hydrogels, and the cells were highly viable after encapsulation in DN hydrogels. Further research into the materials as tissue engineering scaffolds determined that these DN hydrogels weakened when they were prepared in cell-compatible solutions, and the encapsulated cells did not function as well as in gelatin alone.

Motivated by the need to develop better hydrogel system in terms of both mechanical strength and biological properties, we decided to use the microgel-reinforced (MR) hydrogel strategy with the same materials that were used to make the DN hydrogels. MR hydrogels were previously fabricated by embedding stiff microgels into a soft and ductile matrix.^{14, 15} The MR hydrogels exhibited significantly higher strength than the hydrogels with no microgels, and comparable strength to DN hydrogels. The simple difference between MR and DN hydrogels is that the stiff hydrogel is incorporated into the soft and ductile hydrogel as microparticles in MR hydrogels, not as bulk hydrogel as in DN hydrogels. By this difference, we expected two advantages of our MR hydrogels for our purpose. First, although the GG component had to be prepared at relatively low polymer concentrations for DN hydrogels due to the adverse effect of GG/Gelatin mass ratio on the strength of DN hydrogels, for MR hydrogels, GG hydrogels prepared at higher polymer concentration can potentially increase the strength due to their higher stiffness. Second, because cells were encapsulated not in GG but in gelatin, the cells were expected to function better in MR hydrogels than in DN hydrogels.

In this study, we first prepared GG microgels using a water-in-oil emulsion followed by a light-initiated crosslinking. MR hydrogels were prepared by embedding the GG microgels

into gelatin hydrogels and their mechanical properties were examined to compare with those of the DN hydrogels and the gelatin hydrogels with no microgels. MC3T3-E1 preosteoblasts were encapsulated in the MR hydrogels to examine their activity and osteogenic behavior by determining viability, metabolic activity, alkaline phosphatase (ALP) activity, and mineralization. Comparison with DN hydrogels from the same two polymers with the MR hydrogels indicates that the MR hydrogels have better biological performance, and may be of benefit as tissue scaffolds.

2. Materials and methods

2.1. Modification of GG and gelatin

GG (Gelzan™, MW: 1,000,000), gelatin (from porcine skin, Type A), and methacrylic anhydride were purchased from Sigma-Aldrich. Photocrosslinkable GG was prepared by reacting GG with methacrylic anhydride.¹⁶ 3g of GG was dissolved in distilled water at 90°C and the solution was cooled down to 50°C. 24ml of methacrylic anhydride was added to the solution and the reaction was allowed to proceed for 4hrs at 50°C while the pH of the solution was adjusted to 8 by adding 15N NaOH. Then the reaction mixture was dialyzed in distilled water using dialysis membrane (MW cutoff: 12-14kDa, Spectrum Labs, Inc.) at 4°C for 6 days. The solution was frozen and lyophilized to obtain photocrosslinkable GG. The resulting material was kept at -40°C until further use. Similarly, photocrosslinkable gelatin was prepared by reacting gelatin with methacrylic anhydride.¹⁷ 30g of gelatin was dissolved in 300ml of phosphate buffered saline (PBS, 1X, Life Technologies) at 50°C. 3ml of methacrylic anhydride was added to the solution and the reaction was allowed to proceed for 2hrs at 50°C. The reaction mixture was diluted with an equal amount of distilled water and dialyzed in distilled water at 40°C for 6 days. The resulting solution was lyophilized to obtain photocrosslinkable gelatin, and it was kept at -40°C until further use.

2.2. Preparation and characterization of microgels

GG microgels were prepared by using a water-in-oil emulsion.¹⁸ Photocrosslinkable GG was dissolved in ultrapure water containing 1% (w/v) photoinitiator, 2-hydroxy-1-[4-(2-hydroxyethoxy) phenyl]-2-methyl-1-propanone (Irgacure 2959, BASF) at -40°C to make solutions with varying GG concentrations (1.0%, 1.5%, 2.0%, 2.5%, (w/v)). 0.4ml of the GG solution was mixed with 5ml of mineral oil (Sigma-Aldrich) containing 0.02ml of Span 80 (Sigma-Aldrich), and the mixture was homogenized for 3mins by using an OMNI GLH homogenizer (OMNI International). The resulting emulsion was exposed to light (325-500nm, ~7.5mW/cm², EXFO OmniCure S2000) for 120s to obtain crosslinked GG microgels. The resulting solution was dried overnight at -40°C with constant stirring to evaporate the water. GG microgels were separated from mineral oil by centrifugation at 5,000rpm, and washed with isopropanol, hexane, and acetone, before they were dried under vacuum at room temperature for 3 days. The GG microgels were coded as GG1.0, GG1.5, GG2.0, and GG2.5 according to the polymer concentration in the GG microgels.

Scanning electron microscope (SEM) images of dried GG microgels were taken by using a JEOL JSM 6060 SEM with a 2.5kV accelerating voltage at a 10mm working distance. To

prepare specimens, GG microgels were attached onto specimen stubs and sputter coated with gold/palladium (SC7640, Polaron).

Optical microscope images of microgels in PBS were taken by using an optical microscope (Zeiss AxioObserver. D1). The size of microgels in the images was measured by using the ImageJ software.

To measure the swelling ratio, GG microgels were allowed to swell in distilled water for 1hr to reach equilibrium in a tube with known weight. After centrifugation at 5,000rpm, the excessive water was removed and the weight of the wet microgels (W_s) was determined. The microgels were lyophilized and the dry weight (W_d) was determined. The swelling ratio was calculated as W_s/W_d .

2.3. Preparation and characterization of MR and DN hydrogels

GG microgels were allowed to swell in PBS containing 0.05% (w/v) photoinitiator to make solutions with varying GG concentrations (0.25%, 0.5%, 0.75%, 1.0% (w/v)). Photocrosslinkable gelatin was dissolved in these solutions to make 10% (w/v) gelatin solutions with GG microgels. The resulting mixtures were molded into disks with ~8mm diameter and ~1mm thickness, and exposed to light ($\sim 7\text{mW}/\text{cm}^2$) for 180s. The resulting MR hydrogels were immersed in PBS and incubated at 37°C until further experiments. The MR hydrogels were coded as MRx-y, where x is the polymer concentration in the GG microgels, and y is the GG concentration in the MR hydrogels.

DN hydrogels were prepared with only minor modifications from the previously described method.¹² In short, photocrosslinkable GG was dissolved in distilled water containing 0.05% (w/v) photoinitiator at 0.5% (w/v), and the solution was crosslinked with the same method as above. The resulting GG hydrogels were immersed in photocrosslinkable gelatin solution (10% (w/v) in PBS) containing 0.05% (w/v) photoinitiator at 37°C for 1 day. Subsequently, the hydrogels were taken out and the excess gelatin solution was removed from the surface of the hydrogels before they were exposed to light again for 180s. The resulting DN hydrogels were immersed in PBS at 37°C until further experiments.

The polymer concentration of MR hydrogels was determined as W_d/W_s where W_d is the weight of the dried MR hydrogels and W_s is the weight of the swollen MR hydrogels in distilled water. Before W_s was measured, the MR hydrogels were washed with distilled water three times to remove the salts in PBS.

The mechanical properties of hydrogels were determined by unconfined, uniaxial compression tests by using an Instron 5943 mechanical tester. The compression rate was $0.5\text{mm}/\text{min}^{-1}$. The compressive modulus was determined as the slope of the stress-strain curve in the 0-10% strain range. The failure stress was determined as the stress at which the slope of the stress-strain curve started to decrease where the hydrogels started to break.

To observe the microstructure of the hydrogels, SEM images of the cross-section of the hydrogels were taken with a JEOL JSM 6060 SEM with a 5kV accelerating voltage at a 10mm working distance. To minimize changes to the hydrogel structure, the hydrogels were frozen very quickly by liquid nitrogen.¹⁹ After being lyophilized, cross-sections of the

hydrogels were attached onto specimen stubs and sputter coated with gold/palladium (SC7640, Polaron).

2.4. Cell culture and encapsulation

MC3T3-E1 cells were cultured using the growth media, which is Minimum Essential Medium Alpha (MEM Alpha, Life Technologies) supplemented with 10% fetal bovine serum (FBS, Life Technologies) and 1% penicillin-streptomycin (Life Technologies) in 5% CO₂ in air atmosphere at 37°C. Media was replaced every 2-3 days and cells were passaged every 3-4 days when they are 70-80% confluent on the culture flasks.

Photocrosslinkable gelatin solutions (10% (w/v)) with 0.5% and 1.0% of GG1.5 microgels were prepared in PBS containing 0.05% (w/v) photoinitiator at 37°C. Cells were trypsinized and resuspended into these solutions to make 5×10⁶ cells/ml suspensions. The suspensions were pipetted on a Petri dish between two spacers with 600µm thickness and covered with a glass slide. Subsequently they were exposed to light (~7mW/cm²) for 180s to obtain cell-laden MR hydrogels. Similarly, a photocrosslinkable GG solution (1.5% (w/v)) was prepared in PBS containing 0.05% photoinitiator at 37°C, and cell-laden GG hydrogels were prepared with the same method as above. The resulting GG hydrogels were immersed in a photocrosslinkable gelatin solution (10% (w/v) in culture media containing 0.05% photoinitiator) at 37°C for 1day. Then the hydrogels were taken out and the excess gelatin solution was removed from the surface of the hydrogels. The hydrogels were exposed to light (~7mW/cm²) again for 180s to obtain cell-laden DN hydrogels. The resulting cell-laden MR and DN hydrogels were cultured in 5% CO₂ in air atmosphere at 37°C in the differentiation media, which is the growth media supplemented with L-ascorbic acid 2-phosphate sesquimagnesium (50µg/ml) and β-glycerophosphate disodium (10mM)²⁰. The media was replaced every 2-3 days.

2.5. Cell behavior analysis

The cell viability was examined by using a LIVE/DEAD Viability Kit (Life Technologies) according to the manufacturer's instruction. The cell-laden hydrogels stained with calcein AM/ethidium homodimer-1 were visualized with a Nikon Eclipse Ti fluorescence microscope (Nikon), and the cell viability was determined as the number of live cells over the number of all cells.

The metabolic activity was examined by AlamarBlue (Life Technologies) assay. The cell-laden hydrogels were incubated with 300µm AlamarBlue reagent solution (10% (v/v) in growth media) at 37°C for 4hrs. Then the fluorescence (544Ex/590Em) of the solution was measured by using a FLUOstar plate reader (BMG). The reduction of the reagent was calculated as $(F_S - F_B)/(F_S - F_F)$ where F_S is the fluorescence of the sample, F_B is that of the untreated reagent solution, and F_F is that of the 100% reduced solution which was prepared by autoclaving the reagent solution.

ALP activity was measured by using an ALP assay kit (Abcam). The cell-laden hydrogels were disrupted by using a TissueLyser (Qiagen) before 5mM *p*-nitrophenyl phosphate (*p*NPP) solution in the assay buffer was added to the disrupted sample. After incubation for

6hrs at room temperature, the absorbance was measured at 405nm. In order to normalize the ALP activity by the amount of DNA, the DNA was quantified by using a PicoGreen dsDNA Assay Kit (Life Technologies). The disrupted samples were incubated at room temperature for 5mins with the PicoGreen reagent solution in TE buffer before the fluorescence (485Ex/520Em) was measured.

Mineralization was examined by using Alizarin Red S (Sigma-Alrich) according to an Osteogenesis Assay Kit instruction (Millipore). The cell-laden hydrogels were fixed with 4% paraformaldehyde for 30mins, and stained for 5mins with 2% Alizarin Red S solution of which the pH was adjusted to ~4.2 by using 10% acetic acid. Then the hydrogels were washed with distilled water several times to remove all unreacted reagents. The images of the stained samples were taken by using a zoom microscope (Axio Zoom. V16, Zeiss). The samples were then left overnight with 10% acetic acid, heated to 85°C for 10 mins, and neutralized to pH of 4.1-4.5 with 10% ammonium hydroxide. Finally the absorbance was measured at 405nm.

2.6. Statistics

All data were expressed as mean \pm standard deviation. The data were analyzed by using one-way or two-way ANOVA and Bonferroni test to determine statistical significance (GraphPad Prism 5.02, GraphPad Software). Differences were taken to be significant for $p < 0.05$.

3. Results and discussion

Preparation and characterization of microgels

GG molecules consist of rigid repeat units that have many hydroxyl groups available for functionalization with photoreactive methacrylate groups.¹⁶ Thus, hydrogels prepared by photocrosslinking highly methacrylated GG are relatively stiff with the moduli that are $>100\text{kPa}$ at the polymer concentrations of only a few percent, which make them a potentially useful reinforcement material. GG particles were prepared at four different concentrations (1.0%, 1.5%, 2.0%, 2.5%) by using water-in-oil emulsion followed by a light-initiated photocrosslinking (Fig 1). Since the emulsion was not transparent, a high concentration of the photoinitiator (1.0%) was used for the crosslinking. The SEM images of the GG microgels (Fig.2. (A-D)) showed that the resulting microgels were polydisperse and the size of the dried microgels ranged from a few micrometers to hundreds of nanometers. In PBS, the GG microgels swelled and the mean size of particles was measured to be several micrometers (Fig.2. (E-I)). The standard deviation of the size was large due to the high polydispersity of the microgels. No significant difference in the microgel size was observed with increasing the polymer concentration in GG microgels. This is probably because the viscosity of the aqueous GG solution was not high enough to affect the emulsion-forming process, and the GG microgels were highly crosslinked such that their swelling in PBS did not depend strongly on the GG concentration. The swelling ratio of the GG microgels (Fig.2. (J)) decreased as GG concentration increased, which is reasonable because the swollen size in a solution is similar while the polymer concentration increases with GG concentration.

3.2. Preparation and characterization of MR hydrogels

Loosely crosslinked gelatin hydrogels are soft and ductile, with the modulus of a few tens of kPa at 10% polymer concentration. Various amounts of the GG microgels were added to 10% photocrosslinkable gelatin solutions in PBS before the mixture was photocrosslinked to obtain MR hydrogels (Fig.1). The polymer concentration (w/w) of the MR hydrogels increased as the GG concentration in MR hydrogels increased, but no significant difference was observed among different GG concentrations of the microgels (Fig.3. (A)). Although the microgels can serve as additional crosslinks that constrain gelatin molecules from swelling,²¹ thus microgels with different concentrations might have led to different polymer concentrations, the gelatin hydrogels were sufficiently crosslinked that they did not swell appreciably in water, which is presumed to be the reason that microgel formulation did not affect the polymer concentration of the MR hydrogels. It is presumed that the reason that the polymer concentration increased by ~3% with only 1% of GG concentration added in MR hydrogel is that the lower hydrophilicity of GG molecules due to the high degree of methacrylation resulted in the lower water content in the wet state.

The mechanical properties of MR hydrogels were determined by unconfined, uniaxial compression tests. Fig.3. (B) compares the stress-strain curves of two representative MR hydrogels and the gelatin hydrogel with no microgels. When a relatively small amount of microgels was added (MR2.5-0.25 (MR_x-y: GG concentration is x% in microgels and y% in MR hydrogels)), the modulus did not increase significantly, but the failure stress increased significantly (statistical analysis is shown in Fig.3.(C) and (D)). When a relatively large amount of microgels was added (MR2.5-1.0), both the modulus and the failure stress increased significantly, but the failure occurred at a lower strain resulting in not as high failure stress as in the previous formulation (statistical analysis is shown in Fig.3.(C) and (D)). Fig.3. (C) shows the compressive modulus of the all MR hydrogel formulations prepared. GG1.0 microgels were not stiff enough so that adding them with up to 1% GG concentration in MR hydrogel did not make significant increase in the compressive modulus of the MR hydrogels. GG1.5, GG2.0, and GG2.5 microgels did not increase the compressive modulus of the MR hydrogels significantly at only 0.25% GG concentration in MR hydrogel, however, at more than 0.25%, as more amount of the microgels were added, the modulus of MR hydrogels increased. At higher GG concentrations (0.75% and 1%) in MR hydrogel, GG2.5, which is the stiffest microgels, resulted in highest compressive modulus among the all microgel formulations. Fig.3. (D) shows that all formulations of MR hydrogels prepared exhibited higher strength than the gelatin hydrogels. When the microgels of the highest GG concentration (GG2.5) were added, the failure stress abruptly increased at the lowest GG concentration in MR hydrogel (0.25%), and it clearly decreased as the GG concentration in MR hydrogel increased. The maximal strength was 3.2MPa, which was 2.8 times that of the gelatin hydrogels. However, as the GG concentration of the microgels decreased, the failure stress at the lowest GG concentration in MR hydrogel decreased, and it did not decrease as much with the increase of the GG concentration in MR hydrogel. At 1% GG concentration in MR hydrogel, MR hydrogels with GG1.0 showed even higher strength than those with GG2.5. The strengthening mechanism of MR hydrogels has been previously elucidated: the GG microgels provides sacrificial bonds that can resist the crack propagation in the gelatin network¹⁴. Although the GG microgels are brittle, so cracks can

grow in the microgels, the microgels are dispersed in the gelatin network so the cracks of microgels do not propagate into macroscopic ones until the crack of gelatin network starts to grow.

Comparison with DN hydrogels from the same two polymers with MR hydrogels showed that MR hydrogels have significantly higher strength. The compressive modulus and the failure stress of a DN hydrogel were showed in each dotted box in Fig.3. (C) and (D). The formulation of the DN hydrogel was 0.5% GG / 10% gelatin, which is optimal for high strength at 10% gelatin concentration. If the GG concentration increases, the modulus becomes much higher, but the failure stress decreases.¹² But, even with the optimal formulation, the failure stress of the DN hydrogels is only 1.4 times that of the gelatin hydrogels. In previous work, the DN hydrogels were prepared from GG and gelatin solutions in distilled water. However, it turned out that the DN hydrogels prepared from the GG solution in PBS and the gelatin solution in media, which are cell-compatible solutions, exhibited significantly lower strength than those prepared from water solution. We determined that this is because the GG molecules collapse when they are in a solution with high ionic strength such as PBS or media. GG molecules have negative charges on their backbone, so they exist as extended form in distilled water due to the repulsive force between the charges. However, when they are in a solution with many ions, the electric interactions are screened by the ions and the molecules collapse.^{22, 23} The MR hydrogels were also prepared from gelatin solutions with GG microgels in PBS, so the strength might be lower than that of the MR hydrogels prepared form water solutions, but the higher GG concentration of the microgels (thus higher stiffness of microgels) enhanced the strength of the MR hydrogels, which was not the case for the DN hydrogels. This is the mechanical advantage of the MR hydrogels over DN hydrogels.

To investigate the microstructure of the hydrogels, SEM images of the cross-section of the GG, gelatin, DN and MR1.5-1.0 hydrogels were taken (Fig.4). All the hydrogels presented interconnected porous structure, which accelerates the transport of nutrients and waste products. However, except for GG hydrogels, all observed pores were smaller than approximately 10 μ m, so the cell growth and migration in the hydrogels might be impeded. Thus, some degradation of the hydrogels might be needed to facilitate cell behaviors and the formation of extracellular matrix.

3.3. Cell behavior in MR hydrogels

The MC3T3-E1 cell line is a preosteoblast derived from *Mus musculus* (mouse) calvaria.²⁴ It has been widely used as a model to evaluate the capacity of substrates for osteogenic differentiation.²⁵⁻²⁷ It exhibits high levels of differentiation after culture in media with ascorbic acid and phosphate producing osteogenic markers such as ALP and depositing minerals.²⁸⁻³⁰ We encapsulated these cells in five hydrogel formulations which are GG, gelatin, DN, MR1.5-0.5, MR1.5-1.0 (MRx-y: GG concentration is x% in microgels and y% in MR hydrogels) hydrogels. The images of the calcein AM/ethidium homodimer-1 live/dead stained hydrogels are shown in Fig.5. (A). At all formulations of hydrogels, the cell viability was over 70% after 14 days of culture (Fig.5. (B)), which is on par with typical photocrosslinked hydrogels.³¹⁻³³ This shows that the photocrosslinking conditions such as

the intensity of the light, the exposure time and the photoinitiator concentration were well adjusted for the MC3T3-E1 cells. The microgels contained negligible amount of toxic chemicals that could harm cells, and the microgels themselves were not harmful to cells. In addition, requirements for cell survival such as the transport of nutrients and wastes were met. It is presumed that the higher viability in the GG hydrogels than that in other hydrogels at day 7 and 14 is because the initial damage by the photocrosslinking was less in GG hydrogels due to more amount of methacrylate groups which can react with free radicals that is harmful to cells.³¹ It was observed that higher concentration of the photoinitiator led to even lower viability in the gelatin hydrogels, while the viability remained at the same level in the GG hydrogels (data not shown). However, the metabolic activity of the cells showed significant difference between varying formulations as seen in Fig.5. (C). In the gelatin and the two MR hydrogels, the metabolic activity started to increase at day 14, and ended up with about four-fold increase at day 21 compared to day 1. However, the metabolic activity in the GG and the DN hydrogels significantly decreased at day 7, and remained low until day 21. The difference between these two groups was that the cells were encapsulated in gelatin for the former group, while the cells were encapsulated in GG for the latter group. The MC3T3-E1 cells are anchorage-dependent cells of which the activity, function, and differentiation are highly affected by the adhesion to a substrate.^{34, 35} It is well known that gelatin is a great material for this kind of cells because it has many adhesion sites such as RGD peptide.¹⁷ Thus the higher metabolic activity in the former group is presumed that because MC3T3-E1 cells were better attached to the gelatin environment than to the GG environment. Although gelatin molecules penetrated into the GG hydrogel so the cells might face partly the gelatin environment in DN hydrogels, it is speculated that the gelatin could not strongly interact with the cells when the cells were already stuck in the GG network. Seeing that the level of the metabolic activity in the gelatin, MR1.5-0.5, and MR1.5-1.0 hydrogels were all similar, it is concluded that the GG microgels did not interfere significantly with the cell-gelatin interaction at up to 1.0% concentration.

The level of the osteogenic behavior of the MC3T3-E1 cells in each hydrogel formulation was assessed by examining ALP activity and mineralization. As seen in Fig.6, ALP activity in the gelatin and the two MR hydrogels again increased significantly over 21 days of culture, while that in the GG and DN hydrogels remained significantly lower. It is most likely because of the same reason as the difference in metabolic activity, the cell-gelatin interaction. The facilitation of the differentiation of MC3T3-E1 cells or osteogenic differentiation of mesenchymal stem cells (MSCs) by using a cell-adhesive substrate has been shown in previous studies.³⁵⁻³⁷ The enhanced osteogenic behavior in the gelatin and MR hydrogels was also confirmed by the Alizarin Red S staining for minerals (Fig.7, 8). At day 28 of culture, all the surface of the gelatin and the MR hydrogels turned red, while the GG and DN hydrogels still have unstained areas (Fig.7). Quantitative analysis in Fig.8 shows that adding up to 1% of GG microgels into gelatin hydrogels did not affect the amount of the mineralization significantly. Although the amounts of Alizarin Red S stained in the constructs increased at day 21 in all hydrogel formulations compared to those at day 1, the gelatin and the two MR hydrogels contained significantly higher amount of Alizarin Red S than the GG and the DN hydrogels at day 21 and 28. These results show that the MR hydrogel is a better system than the DN hydrogel in perspective of biological properties as

well. However, it should be noted that depending on the properties of the cells encapsulated, the effect of the hydrogel formulation on the function or the differentiation of the cells can be different. For example, RGD peptides that exist on gelatin molecules promote early stages of chondrogenesis of MSCs, but their persistence in the scaffold can limit complete differentiation of MSCs.^{38, 39} Thus, the properties of the cells always need to be considered when a hydrogel formulation is selected for a certain purpose. Finding other materials that have different biological properties and can be used as the stiff reinforcing microgels or the soft and ductile matrix will thus broaden the range of applications of MR hydrogels.

Finally, another advantage of MR hydrogels as tissue scaffolds is that they are potentially injectable as previously studied photocrosslinkable polymers,^{40, 41} which is not the case for DN hydrogels. By adding the GG component in the gelatin hydrogels as microgels not as bulk hydrogels, injection of the gelatin solutions with GG microgels and cells into a body followed by a photocrosslinking *in situ* became possible. This enables the minimally invasive implantation, which is one of the advantages of hydrogel-based tissue scaffolds over those from different types of material.^{1, 40, 42} However, it should be noted that, although the feasibility of photocrosslinking of injected polymers *in vivo* by transdermal light exposure was confirmed,^{43, 44} further studies to overcome inefficient light penetration through skin and develop biocompatible photoinitiators are needed for clinical use as injectable tissue scaffolds.

4. Conclusion

We developed mechanically strong MR hydrogels by embedding stiff GG microgels into soft and ductile gelatin hydrogels. The MR hydrogels exhibited higher strength than the DN hydrogels and the gelatin hydrogels with no microgels. The strength of MR hydrogels varied with the polymer concentration in the GG microgels and the GG concentration in the MR hydrogels. MC3T3-E1 preosteoblasts were encapsulated in the MR hydrogels with a high cell viability. They exhibited as high metabolic activity in the MR hydrogels as in the gelatin hydrogels after culture, while their metabolic activity remained low over time in the DN hydrogels. The osteogenic behavior determined by measuring ALP activity and mineralization was facilitated as greatly in the MR hydrogels as in the gelatin hydrogels, while the osteogenic behavior was not as facilitated in DN hydrogels. These results suggest that the MR hydrogels may have high potential as load-bearing tissue scaffolds.

Acknowledgments

Hyeongho Shin acknowledges financial support from the Samsung Scholarship. This paper was supported by the National Institutes of Health (HL092836, DE021468, EB02597, AR057837), the National Science Foundation CAREER award (DMR0847287). The authors would like to thank Dr. Jesper Hjortnaes and Silvia Mihaila for helping with biological assays, and Dr. Akhilesh Gaharwar for helping with the zoom microscope.

References

1. Drury JL, Mooney DJ. *Biomaterials*. 2003; 24:4337–4351. [PubMed: 12922147]
2. Lee K, Mooney D. *Chemical reviews*. 2001; 101:1869–1880. [PubMed: 11710233]
3. Peppas N, Hilt J, Khademhosseini A, Langer R. *Advanced Materials*. 2006; 18:1345–1360.
4. Gong J, Katsuyama Y, Kurokawa T, Osada Y. *Advanced Materials*. 2003; 15:1155–1158.

5. Nakayama A, Kakugo A, Gong JP, Osada Y, Takai M, Erata T, Kawano S. *Advanced Functional Materials*. 2004; 14:1124–1128.
6. Weng L, Gouldstone A, Wu Y, Chen W. *Biomaterials*. 2008; 29:2153–2163. [PubMed: 18272215]
7. Okumura Y, Ito K. *Advanced Materials*. 2001; 13:485–487.
8. Haraguchi K, Takehisa T. *Advanced Materials*. 2002; 14:1120–1124.
9. Sakai T, Matsunaga T, Yamamoto Y, Ito C, Yoshida R, Suzuki S, Sasaki N, Shibayama M, Chung UI. *Macromolecules*. 2008; 41:5379–5384.
10. Henderson KJ, Zhou TC, Otim KJ, Shull KR. *Macromolecules*. 2010; 43:6193–6201.
11. Glassman MJ, Chan J, Olsen BD. *Advanced Functional Materials*. 2013; 23:1182–1193.
12. Shin H, Olsen BD, Khademhosseini A. *Biomaterials*. 2012; 33:3143–3152. [PubMed: 22265786]
13. Na YH, Kurokawa T, Katsuyama Y, Tsukeshiba H, Gong JP, Osada Y, Okabe S, Karino T, Shibayama M. *Macromolecules*. 2004; 37:5370–5374.
14. Hu J, Hiwatashi K, Kurokawa T, Liang SM, Wu ZL, Gong JP. *Macromolecules*. 2011; 44:7775–7781.
15. Hu J, Kurokawa T, Hiwatashi K, Nakajima T, Wu ZL, Liang SM, Gong JP. *Macromolecules*. 2012; 45:5218–5228.
16. Coutinho DF, Sant SV, Shin H, Oliveira JT, Gomes ME, Neves NM, Khademhosseini A, Reis RL. *Biomaterials*. 2010; 31:7494–7502. [PubMed: 20663552]
17. Nichol JW, Koshy ST, Bae H, Hwang CM, Yamanlar S, Khademhosseini A. *Biomaterials*. 2010; 31:5536–5544. [PubMed: 20417964]
18. Jia XQ, Yeo Y, Clifton RJ, Jiao T, Kohane DS, Kobler JB, Zeitels SM, Langer R. *Biomacromolecules*. 2006; 7:3336–3344. [PubMed: 17154461]
19. Shen Z, Bi J, Shi B, Nguyen D, Xian CJ, Zhang H, Dai S. *Soft Matter*. 2012; 8:7250–7257.
20. Fernandes H, Dechering K, Van Someren E, Steeghs I, Apotheker M, Leusink A, Bank R, Janeczek K, Van Blitterswijk C, de Boer J. *Tissue Engineering Part A*. 2009; 15:3857–3867. [PubMed: 19694522]
21. Hu J, Kurokawa T, Hiwatashi K, Nakajima T, Wu ZL, Liang SM, Gong JP. *Macromolecules*. 2012; 45:5218–5228.
22. Takahashi A, Kato T, Nagasawa M. *The Journal of Physical Chemistry*. 1967; 71:2001–2010.
23. Nagasawa M, Eguchi Y. *The Journal of Physical Chemistry*. 1967; 71:880–888.
24. Sudo H, Kodama HA, Amagai Y, Yamamoto S, Kasai S. *Journal of Cell Biology*. 1983; 96:191–198. [PubMed: 6826647]
25. Lee YK, Song J, Lee SB, Kim KM, Choi SH, Kim CK, LeGeros RZ, Kim KN. *Journal of Biomedical Materials Research Part A*. 2004; 69A:188–195. [PubMed: 14999767]
26. Isama K, Tsuchiya T. *Biomaterials*. 2003; 24:3303–3309. [PubMed: 12763458]
27. Khatiwala CB, Peyton SR, Putnam AJ. *American Journal of Physiology-Cell Physiology*. 2006; 290:C1640–C1650. [PubMed: 16407416]
28. Quarles LD, Yohay DA, Lever LW, Caton R, Wenstrup RJ. *Journal of Bone and Mineral Research*. 1992; 7:683–692. [PubMed: 1414487]
29. Wang D, Christensen K, Chawla K, Xiao GZ, Krebsbach PH, Franceschi RT. *Journal of Bone and Mineral Research*. 1999; 14:893–903. [PubMed: 10352097]
30. Franceschi RT, Iyer BS, Cui Y. *Journal of Bone and Mineral Research*. 1994; 9:843–854. [PubMed: 8079660]
31. Fedorovich NE, Oudshoorn MH, van Geemen D, Hennink WE, Alblas J, Dhert WJA. *Biomaterials*. 2009; 30:344–353. [PubMed: 18930540]
32. Burdick J, Chung C, Jia X, Randolph M, Langer R. *Biomacromolecules*. 2005; 6:386–391. [PubMed: 15638543]
33. Bae H, Ahari AF, Shin H, Nichol JW, Hutson CB, Masaeli M, Kim SH, Aubin H, Yamanlar S, Khademhosseini A. *Soft Matter*. 2011; 7:1903–1911. [PubMed: 21415929]
34. Wang C, Varshney RR, Wang D-A. *Advanced Drug Delivery Reviews*. 2010; 62:699–710. [PubMed: 20138940]
35. Sun J, Xiao WQ, Tang YJ, Li KF, Fan HS. *Soft Matter*. 2012; 8:2398–2404.

36. Salasnyk RM, Williams WA, Boskey A, Batorsky A, Plopper GE. *Journal of Biomedicine and Biotechnology*. 2004;24–34. [PubMed: 15123885]
37. Chastain SR, Kundu AK, Dhar S, Calvert JW, Putnam AJ. *Journal of Biomedical Materials Research Part A*. 2006; 78A:73–85. [PubMed: 16602124]
38. Salinas CN, Anseth KS. *Biomaterials*. 2008; 29:2370–2377. [PubMed: 18295878]
39. Salinas CN, Cole BB, Kasko AM, Anseth KS. *Tissue Engineering*. 2007; 13:1025–1034. [PubMed: 17417949]
40. Burdick JA, Anseth KS. *Biomaterials*. 2002; 23:4315–4323. [PubMed: 12219821]
41. Jia X, Burdick JA, Kobler J, Clifton RJ, Rosowski JJ, Zeitels SM, Langer R. *Macromolecules*. 2004; 37:3239–3248.
42. Tan HP, Chu CR, Payne KA, Marra KG. *Biomaterials*. 2009; 30:2499–2506. [PubMed: 19167750]
43. Hillel AT, Unterman S, Nahas Z, Reid B, Coburn JM, Axelman J, Chae JJ, Guo Q, Trow R, Thomas A. *Science Translational Medicine*. 2011; 3:93ra67–93ra67.
44. Lin R-Z, Chen Y-C, Moreno-Luna R, Khademhosseini A, Melero-Martin JM. *Biomaterials*. 2013; 34:6785–6796. [PubMed: 23773819]

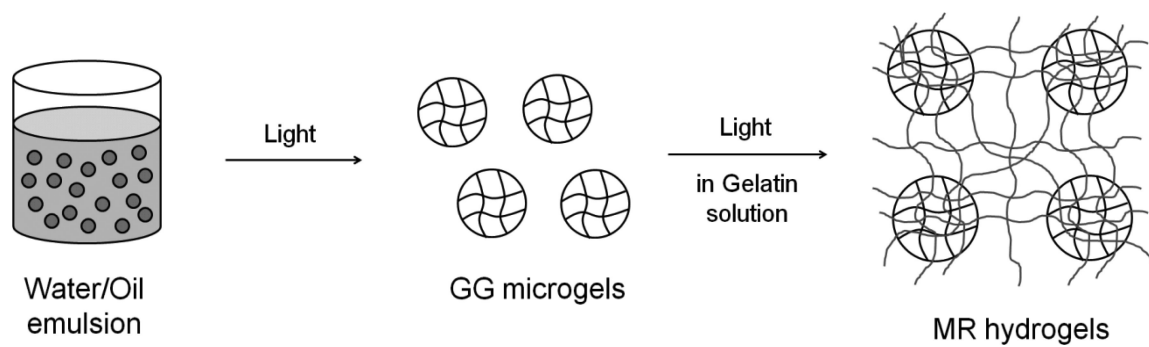


Fig. 1.
Preparation procedure of MR hydrogels.

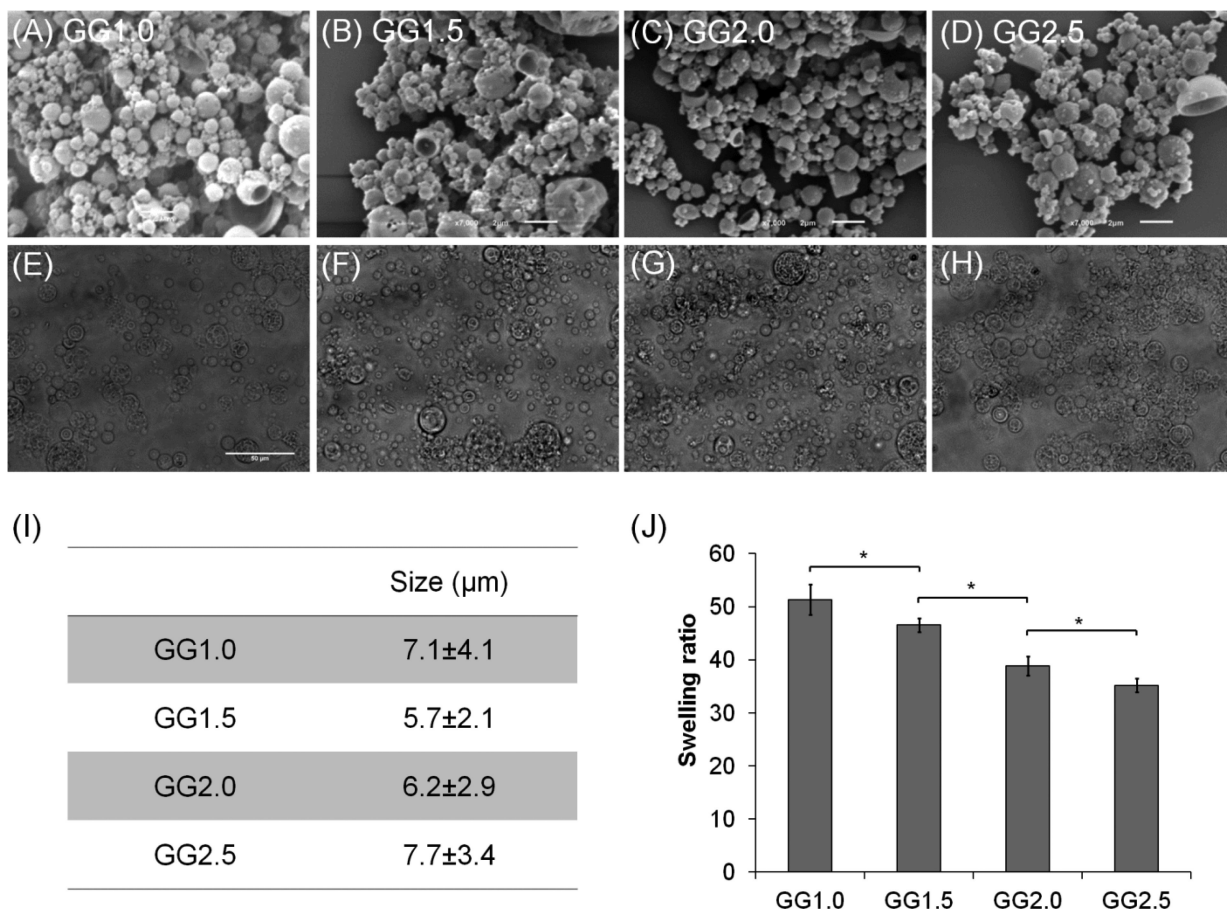


Fig. 2. SEM (A-D) and optical microscope images (E-H) of GG microgels prepared at different polymer concentrations: (A,E) GG1.0, (B,F) GG1.5, (C,G) GG2.0 (D,H) GG2.5. The scale bars in (A-D) represent $2\mu\text{m}$, and the scale bar in (E) represents $50\mu\text{m}$. (I) Particle size of GG microgels in PBS. (J) Swelling ratio of GG microgels in distilled water. (*) indicates significant difference ($p < 0.05$).

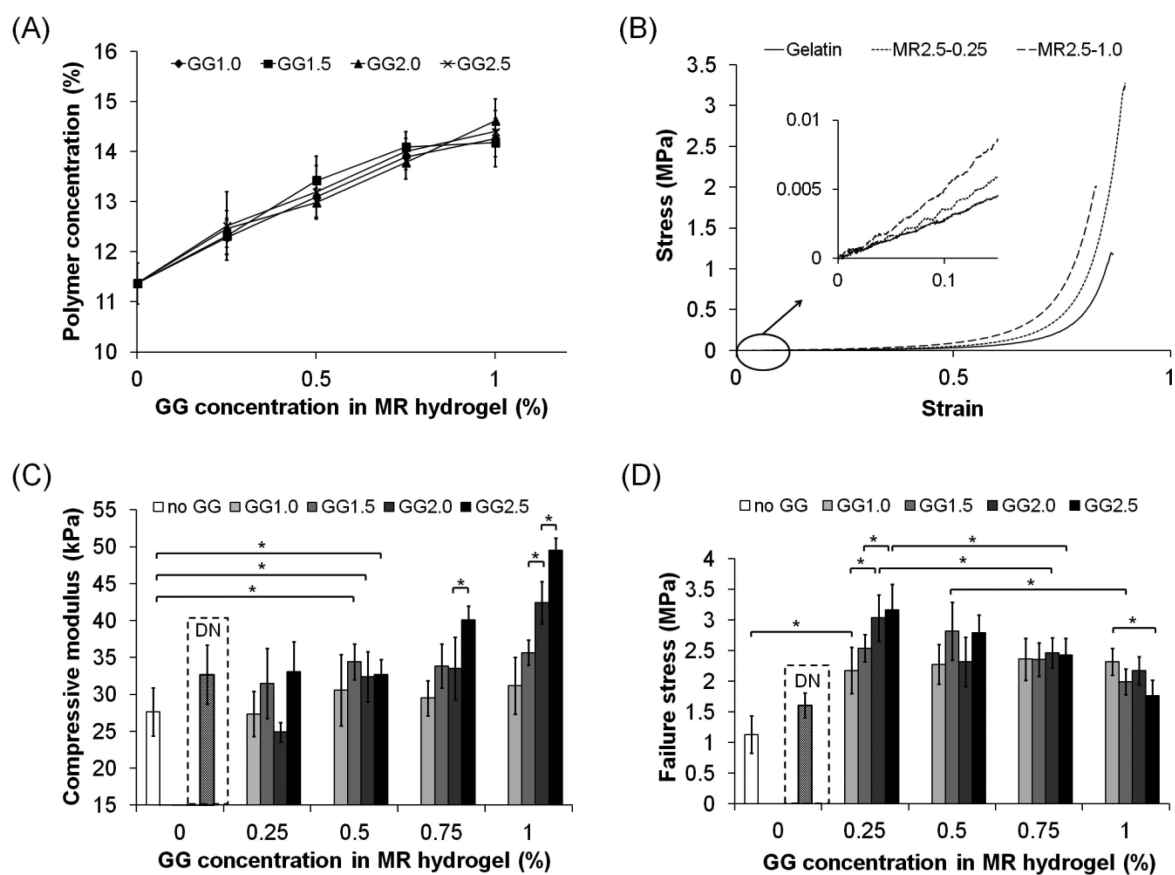


Fig. 3. Polymer concentration of MR hydrogels (A) and mechanical properties of gelatin and MR hydrogels: (B) stress-strain curve (MRx-y: GG concentration is x% in microgels and y% in MR hydrogels), (C) compressive modulus and (D) failure strength. Compressive modulus and failure stress of DN hydrogels are added for comparison in (C) and (D) in each dotted box. (*) indicates significant difference ($p < 0.05$).

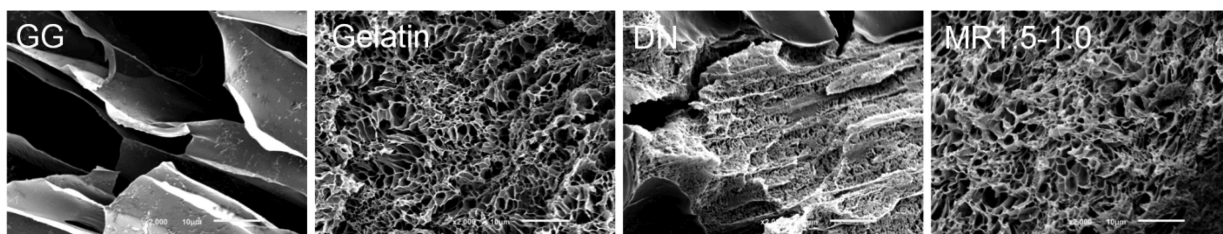
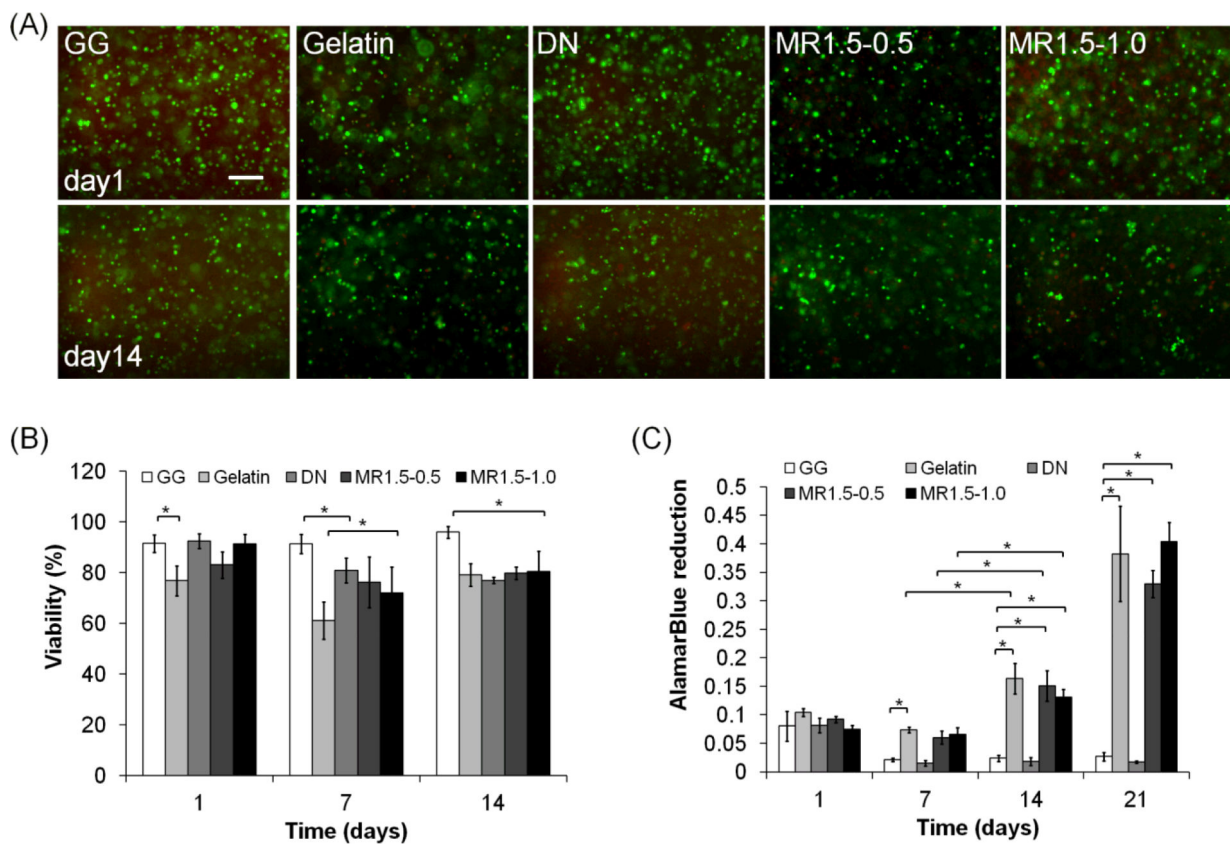


Fig. 4.
SEM images of cross-section of hydrogels. The scale bars represent 10 μ m.

**Fig. 5.**

(A) Live/dead staining on MC3T3-E1 cells / hydrogel constructs after 1 and 14 days in culture. The scale bar represents 100 μ m. (B) Viability and (C) metabolic activity (AlamarBlue assay) of MC3T3-E1 cells encapsulated in hydrogels after culture. (*) indicates significant difference ($p < 0.05$).

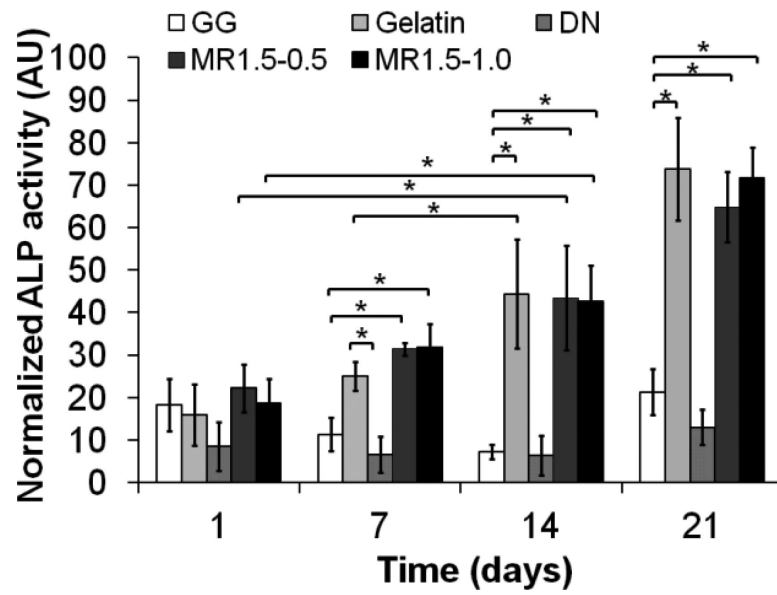


Fig. 6. Alkaline phosphatase expression of MC3T3-E1 cells normalized by the amount of DNA after culture. (*) indicates significant difference ($p < 0.05$).

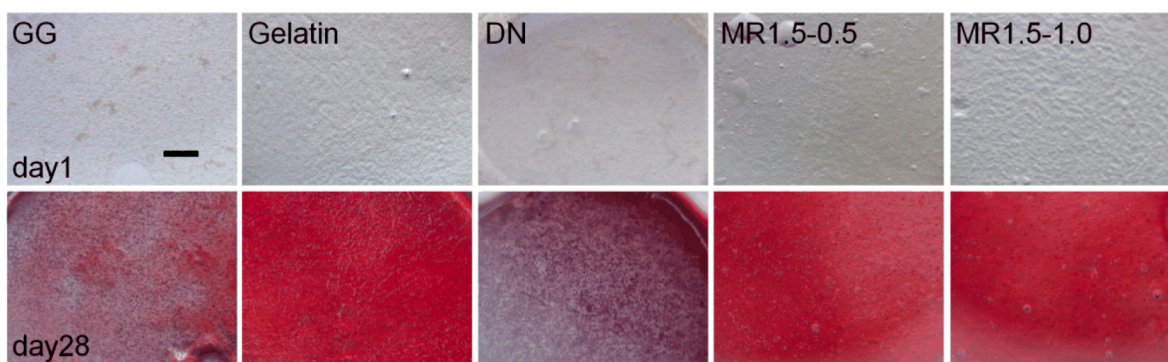


Fig. 7. Alizarin Red S staining on MC3T3-E1 cells / hydrogel constructs after 1 and 28 days in culture. The scale bar represents 500 μ m.

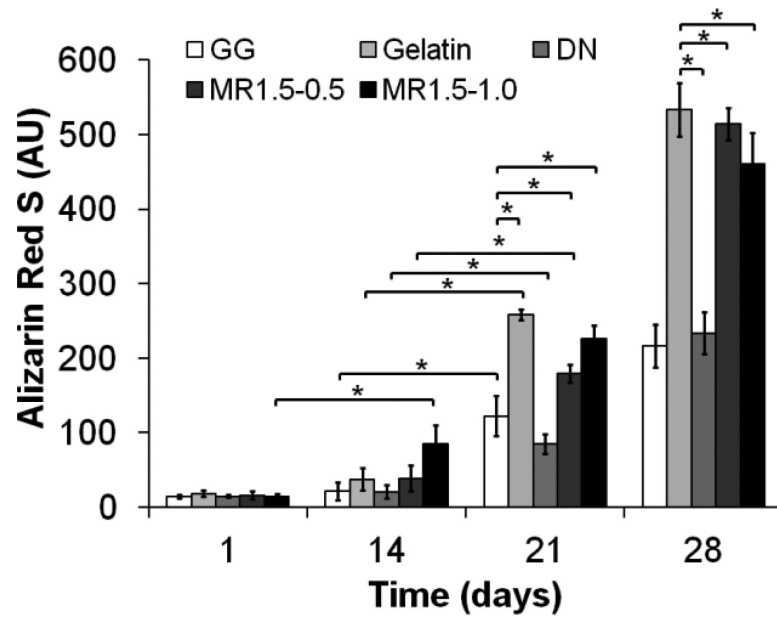


Fig. 8. Quantification of Alizarin Red S stained in MC3T3-E1 cells / hydrogel constructs. (*) indicates significant difference ($p < 0.05$).